

# Chirping of an MMI-PHASAR Demultiplexer for Application in Multiwavelength Lasers

C. G. P. Herben, C. G. M. Vreeburg, X. J. M. Leijtens, H. Blok, *Member, IEEE*, F. H. Groen, I. Moerman, J. W. Pedersen, and M. K. Smit, *Associate Member, IEEE*

**Abstract**—We report the first chirped multimode interference-based phased-array (MMI-PHASAR) for application in multiwavelength lasers (MWL's). To avoid wavelength ambiguity in MWL's, undesired orders are suppressed by chirping the array of arms in the demultiplexer. Simulations show that a suppression of adjacent orders of more than 2 dB can be achieved. A  $1 \times 5$  MMI-PHASAR has been realized in which the effect of the chirping is clearly visible according to the simulations.

**Index Terms**—Demultiplexing, integrated optics, MMI-PHASAR, semiconductor waveguides, wavelength-division multiplexing.

## I. INTRODUCTION

A KEY COMPONENT in wavelength-division multiplexing (WDM) networks is the multiwavelength source. Recently, several configurations of multiwavelength lasers (MWL's) have been reported. One approach uses an array of wavelength selective lasers combined into one output with a starcoupler [1], [2]. However, the use of a starcoupler as combiner introduces high coupling losses. Another approach that avoids this loss uses a wavelength selective filter inside the laser cavity [3]–[5]. Up to now, phased-array (PHASAR) and grating demultiplexers have been used as wavelength selective device in MWL's. In this letter we report on the performance of a compact low loss chirped multimode interference-based phased-array (MMI-PHASAR) [6] as wavelength selective filter. Inherent to the MMI-PHASAR is its periodical response: the free spectral range equals the number of outputs times the channel spacing (channel “wrap-around”). When the MMI-PHASAR is used in a MWL, the device will start lasing in the order which is closest to the maximum of the amplifier gain spectrum. If a channel and its adjacent order have equal distance to the gain maximum, the laser may start lasing at the wavelength of the adjacent order. To avoid wavelength ambiguity, the demultiplexer response of undesired orders should be suppressed. A method for altering the response of a conventional PHASAR has been proposed by Doerr [7] and

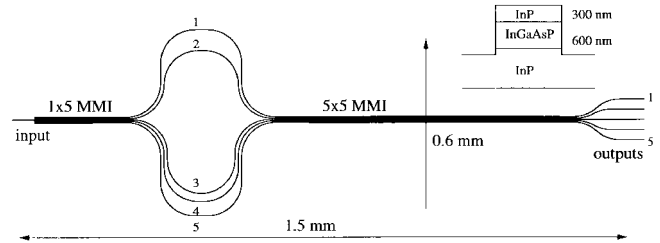


Fig. 1. Layout of  $(1 \times 5)$  MMI-PHASAR demultiplexer.

TABLE I  
ARM LENGTH DIFFERENCES RELATIVE TO THE SHORTEST ARM

	Normal	Chirped
Arm 1 ( $i=4$ )	$3\Delta L$	$3\Delta L - 45\lambda_c$
Arm 2 ( $i=1$ )	0	0
Arm 3 ( $i=2$ )	$\Delta L$	$\Delta L - 30\lambda_c$
Arm 4 ( $i=3$ )	$2\Delta L$	$2\Delta L - 45\lambda_c$
Arm 5 ( $i=5$ )	$4\Delta L$	$4\Delta L - 30\lambda_c$

demonstrated in a MWL [8]. It consists of chirping of the demultiplexer by changing the arm lengths. A similar approach is applied here to chirp the MMI-PHASAR.

## II. PRINCIPLE OF OPERATION

An  $N$ -channel MMI-PHASAR consists of two MMI-couplers connected by  $N$  waveguide arms of unequal length (see Fig. 1). The MMI-PHASAR uses a  $1 \times N$  MMI-splitter that equally divides the light over the  $N$  arms and a  $N \times N$  MMI-coupler recombines the light. With a proper choice of the arm lengths (see Table I) as discussed in [6], [9], [10], light with different wavelengths will be demultiplexed to different outputs. The chirping of the demultiplexer is done by adjusting the arm length differences. The desired effect of the chirp is the alteration of the passband envelope in such a way that the response decreases for unwanted wavelengths. The effect of the chirp can be seen as a multiplication of the passband envelope and a window function, the chirp envelope. The position and width of this chirp envelope has to be chosen in such a way that only the desired order will be transmitted. If the length of an arm is changed by a multiple of a certain chirp wavelength divided by the effective index,  $\lambda_c/n_{\text{eff}}$ , this will not affect the response for this specific wavelength. However, for wavelengths different from this chirp wavelength,  $\lambda_c$ , the phases will no longer satisfy the

Manuscript received March 11, 1997; revised April 28, 1997. This work was supported in part by the ACTS AC-065 under Project BLISS.

C. G. P. Herben, C. G. P. Vreeburg, X. J. M. Leijtens, H. Blok, and M. K. Smit are with Department of Electrical Engineering, Delft University of Technology, NL-2600 GA Delft, The Netherlands.

F. H. Groen is with Delft University of Technology, Department of Physics. I. Moerman is with University of Gent, IMEC, Gent, Belgium.

J. W. Pedersen is with KPN Research, Leidschendam, The Netherlands.

Publisher Item Identifier S 1041-1135(97)05682-6.

required phase relations [11] and the response will degrade. In a normal nonchirped MMI-PHASAR the length difference between two arms is constant as in equation 1. Using the shortest set of armlengths that satisfy the necessary relations the length increases from arm 2 via arms 3,4,1 to arm 5 (Fig. 1). In other words the armlength increment does not coincide with the sequential positions of the arms. In the equations  $i$  ( $i = 1, \dots, N$ ) stands for the length increment rather than the position of the arms.

$$l_{i+1} - l_i = \Delta L, \quad (1)$$

In the chirped MMI-PHASAR, we change the length differences linearly with the arm length according to

$$l_{i+1} - l_i = \Delta L + \gamma \left( i - \frac{N+1}{2} \right) \lambda_c \quad (2)$$

with  $\lambda_c$  the chirp wavelength inside the material, determining the position of the chirp envelope and  $\gamma$  an integer constant to adjust the width of the envelope. Linear chirp is used since simulations show that higher order chirp functions usually lead to small repetition periods of the chirp envelope and thus destroy the desired effect. Application of more complex functions to overcome this problem is not feasible due to the limited number of arms in a MMI-PHASAR. The number of arms could be increased by adding dummy ports to the MMI-PHASAR, however the MMI-couplers length increases quadratically with the width, thus, rapidly increasing the device size.

### III. DESIGN AND FABRICATION

A five-channel MMI-PHASAR was designed for application in a four-channel MWL. The fifth channel is used as a dummy channel for increasing the distance between adjacent orders. This is necessary to get sufficient suppression of the adjacent orders relative to the main desired order. The layout of the  $1 \times 5$  MMI-PHASAR is depicted in Fig. 1. The  $1 \times 5$  MMI-splitter measures  $19.8 \times 172 \mu\text{m}^2$ , the  $5 \times 5$  MMI-coupler measures  $19.8 \times 686 \mu\text{m}^2$  and the arm length difference  $\Delta L = 38.8 \mu\text{m}$ , resulting in a channel spacing of 3.2 nm. The total device measures only  $1.5 \times 0.6 \text{ mm}^2$ . The chip was fabricated in a MOVPE grown layer stack consisting of a 600-nm-thick InGaAsP( $\lambda_{\text{gap}} = 1.3 \mu\text{m}$ ) film layer and a 300 nm InP cladding layer on an InP substrate as depicted in Fig. 1. A 100-nm-thick PECVD-SiN<sub>x</sub> layer served as an etching mask for the waveguides. The pattern was defined using contact UV-exposure with positive photoresist and transferred in the SiN<sub>x</sub>-layer by CHF<sub>3</sub> reactive ion etching. The waveguides were deeply etched employing a CH<sub>4</sub>-H<sub>2</sub> etching and O<sub>2</sub> descumming process, optimized for low losses [12].

Propagation losses for 2- $\mu\text{m}$ -wide straight waveguides are 2–2.5 dB/cm for TE polarized light. Bends with 100- $\mu\text{m}$  radius were used. Two types of MMI-PHASAR were fabricated; one nonchirped and one chirped in which the arm lengths were changed according to (2) with  $N = 5$  and  $\gamma = 15$ . In Table I,

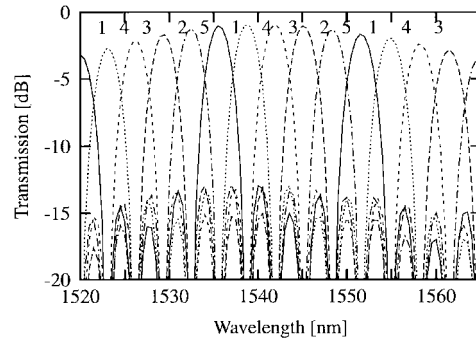


Fig. 2. Simulated response of the nonchirped device.

the resulting arm lengths are given with  $\lambda_c$  the desired center wavelength of the chirp envelope.

The amount of chirp was determined by simulating the demultiplexer response using a CAD-tool for photonic integrated circuits [13]. The devices were measured using the spontaneous emission spectrum of an EDFA as a broad-band light source and a microscope objective to launch the light into the chip. The light was collected with a tapered fiber and analyzed using an optical spectrum analyzer.

### IV. TOLERANCES

Experimental results of MMI-PHASARS reported so far show high crosstalk and nonuniformities. The major reason for this are the stringent demands on the processing in order to make the device operate properly. In the MMI-PHASAR presented here several techniques have been applied to relax these processing demands.

In order to minimize the nonuniformities caused by differences in loss in the various arms of the array, the arms have been constructed using the same number of curves and equal radii of curvature. The length differences have been introduced in straight sections only. Furthermore, a deeply etched structure is used which allows not only for small device dimensions, but also reduces the effect of nonuniform etching along the wafer.

The waveguides have been tapered from 2 to 3  $\mu\text{m}$  at the input and outputs of the MMI's to make these less sensitive to width variations [14]. Without using tapers less than 1 dB loss penalty requires MMI dimensions accurate within  $\pm 0.1 \mu\text{m}$ . Using tapers this requirement is relaxed to  $\pm 0.18 \mu\text{m}$ .

### V. EXPERIMENTAL RESULTS

Figs. 2 and 3 show an experimental and a simulated response of the normal  $1 \times 5$  MMI-PHASAR, respectively. The numbers above the curves denote the outputs. The figure shows a simulated response optimized for a central wavelength of 1540 nm. The minimum excess loss is approximately 1 dB caused by offsets between straight and curved waveguides and losses of the MMI-couplers. The fall-off as a function of the wavelength is caused by the wavelength dependence of the MMI's. The crosstalk at the maxima of the passbands is less than -20 dB.

In the experimental response, the losses are slightly higher and the optimum of the response is shifted about 10 nm toward

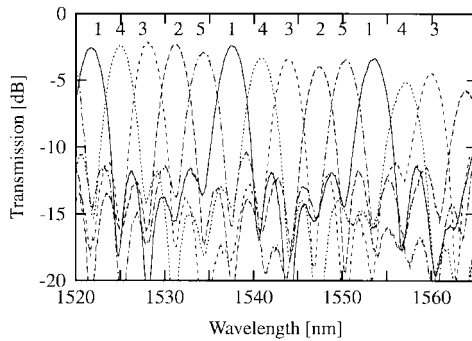


Fig. 3. Measured response of the nonchirped device.

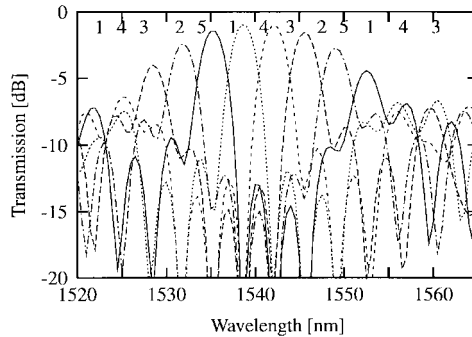


Fig. 4. Simulated response of the chirped device.

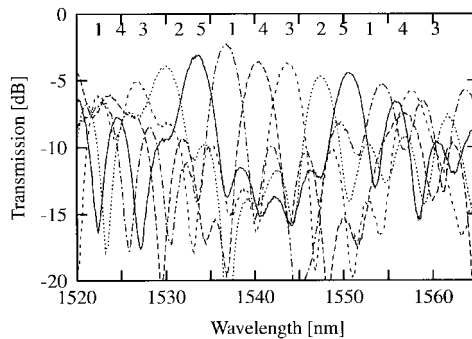


Fig. 5. Measured response of the chirped device.

shorter wavelengths. This shift is mainly due to deviations in the absolute thicknesses and composition of the layer stack. Measured crosstalk is about  $-12$  dB and the channel uniformity, within one order, is better than 1 dB. Figs. 4 and 5 show the simulated and experimental response of the chirped MMI-PHASAR demultiplexer. From the simulation it can be seen, that suppression of the adjacent orders of at least 2 dB is achieved if channel five is not used. This fifth channel has two nearly equal passbands since the center of the chirp envelope lies exactly between these two peaks. In the experimental results, the effect of the chirping is clearly visible. The suppression is not as effective as in the simulation mainly due to nonuniformities that are also visible in the nonchirped response. Since the optimum of the nonchirped response is shifted away from the design wavelength, the

optimum transmission of the MMI's does no longer coincides with the center of the chirp envelope. Qualitatively, however, the experimental results agree very well with the simulated results.

## VI. CONCLUSION

A  $1 \times 5$  MMI-PHASAR has been demonstrated of which the undesired orders are suppressed by applying a linear chirp to the arm lengths. Simulation predicts a suppression of at least 2 dB. Due to a shift in wavelength response the experimentally obtained suppression is less. However, the experiments clearly show the effect of the chirp and are in good agreement with the simulations.

## REFERENCES

- [1] M. Young, U. Koren, B. Miller, M. Newkirk, M. Chien, M. Zirngibl, C. Dragone, B. Tell, H. Presby, and G. Raybon, "A  $16 \times 1$  wavelength division multiplexer with integrated distributed bragg reflector lasers and electroabsorption modulators," *IEEE Photon. Technol. Lett.*, vol. 5, pp. 908–910, Aug. 1993.
- [2] C. Zah, M. Amersfoort, B. Pathak, F. Favire, P. Lin, A. Rajhel, N. Andreadakis, R. Bhat, C. Caneau, and M. Koza, "Wavelength accuracy and output power of multiwavelength DFB laser arrays with integrated star couplers and optical amplifiers," *IEEE Photon. Technol. Lett.*, vol. 8, pp. 864–866, July 1996.
- [3] M. Zirngibl, C. Joyner, C. Doerr, L. Stulz, and H. Presby, "An 18-channel multifrequency laser," *IEEE Photon. Technol. Lett.*, vol. 8, pp. 870–872, July 1996.
- [4] A. Staring, L. Spiekman, J. Binsma, E. Jansen, T. van Dongen, P. Thijs, M. Smit, and B. Verbeek, "A compact nine-channel multiwavelength laser," *IEEE Photon. Technol. Lett.*, vol. 8, pp. 1139–1141, Sept. 1996.
- [5] K. Poguntke, J. Soole, A. Scherer, H. LeBlanc, C. Caneau, R. Bhat, and M. Koza, "Simultaneous multiple wavelength operation of a multistripe array grating integrated cavity laser," *Appl. Phys. Lett.*, vol. 62, pp. 2024–2026, Apr. 1993.
- [6] C. van Dam, M. Amersfoort, G. ten Kate, F. van Ham, M. Smit, P. Besse, M. Bachmann, and H. Melchior, "Novel InP-based phased-array wavelength demultiplexer using a generalized MMI-MZI configuration," in *Proc. 7th Conf. Integrated Optics (ECIO '95)*, Delft, The Netherlands, 1995, pp. 275–278.
- [7] C. Doerr, M. Zirngibl, and C. Joyner, "Chirping of the waveguide grating router or free-spectral-range mode selection in the multifrequency laser," *IEEE Photon. Technol. Lett.*, vol. 8, pp. 500–502, Apr. 1996.
- [8] C. Doerr, C. Joyner, M. Zirngibl, and L. Stulz, "Chirped waveguide grating router multifrequency laser with absolute wavelength control," *IEEE Photon. Technol. Lett.*, vol. 8, pp. 1606–1608, Dec. 1996.
- [9] L. Lierstuen and A. Sudbø, "8-channel wavelength division multiplexer based on multi-mode interference couplers," *IEEE Photon. Technol. Lett.*, vol. 7, pp. 1034–1036, Sept. 1995.
- [10] P. Besse, M. Bachmann, C. Nadler, and H. Melchior, "The integrated prism interpretation of multileg Mach-Zehnder interferometers based on multimode interference couplers," *Opt. Quantum Electron.*, vol. 27, pp. 909–920, Oct. 1995.
- [11] M. Bachmann, P. Besse, and H. Melchior, "General self-imaging properties in  $N \times N$  multimode interference couplers including phase relations," *Appl. Opt.*, vol. 33, pp. 3905–3911, June 1994.
- [12] Y. Oei, L. Spiekman, F. Groen, I. Moerman, E. Metaal, and J. Pedersen, "Novel RIE-process for high quality InP-based waveguide structures," in *Proc. 7th Conf. Integrated Optics (ECIO '95)*, Delft, The Netherlands, 1995, pp. 205–208.
- [13] X. Leijtens, P. Le Lourec, and M. Smit, "S-matrix oriented CAD-tool for simulating complex integrated optical circuits," *J. Select. Topics Quantum Electron.*, vol. 2, pp. 257–262, June 1996.
- [14] P. A. Besse, M. Bachmann, H. Melchior, L. B. Soldano, and M. K. Smit, "Optical band-width and fabrication tolerances of multimode interference couplers," *J. Lightwave Technol.*, vol. 12, pp. 1004–1009, June 1994.